NDT&E International 68 (2014) 33–42

Contents lists available at ScienceDirect

NDT&E International

journal homepage: www.elsevier.com/locate/ndteint

Influence of rebars on elastic-wave-based synthetic aperture focusing technique images for detecting voids in concrete structures

Jian-Hua Tong [a], Chin-Lung Chiu [b,*], Chung-Yue Wang [c], Shu-Tao Liao [d]

[a] Department of Computer Science and Information Engineering, Hungkuang University, Taichung 433, Taiwan
[b] Department of Construction Engineering, National Taiwan University of Science and Technology, Taipei 106, Taiwan
[c] Department of Civil Engineering, National Central University, Tao-Yuan 320, Taiwan
[d] Department of Civil Engineering, Chung Hua University, Hsinchu 300, Taiwan

ARTICLE INFO

Article history:
Received 11 March 2014
Received in revised form
4 July 2014
Accepted 4 August 2014
Available online 17 August 2014

Keywords:
Elastic wave
Imaging
Nondestructive testing (NDT)
Synthetic aperture focusing technique (SAFT)
Impact-echo method

ABSTRACT

Using elastic-wave-based NDT methods to detect defects in RC structures is difficult because of the interference of rebars. In this study, the interference effect on the quality of SAFT images was quantitatively explored using a series of numerical simulations. Furthermore, two concrete specimens were fabricated for experimental verification. The experimental results exhibited strong agreement with those of quantitative analyses used in numerical simulations. These results indicated that using SAFT images to expose the defects under a layer of rebars is feasible. Moreover, a useful guideline for selecting the impacting source to produce a high-quality SAFT image is proposed.

1. Introduction

Elastic-wave-based nondestructive testing (NDT) technologies [1] have been used widely to evaluate the integrity of concrete structures. The key to the success of such tests is the point-source/point-receiver scheme, which involves using a mechanical impactor to generate high-powered elastic waves. This scheme is especially suitable for in situ applications because it enables the limitation of the functioning depth caused by conventional ultrasonic probes, which use low power to be overcome. In 1986, Carino et al. proposed a point-source/point-receiver pulse-echo technique for detecting flaws in concrete and subsequently initiated the evolution of the impact-echo method [2–4]. Since 1995, Wu et al. have proposed a series of methods to determine the elastic constants and depths of surface-breaking cracks in concrete elements by using transient elastic waves [5–10]. They have demonstrated the capability of using these methods to detect simple defects in concrete elements. However, successful results are frequently difficult to obtain if only a single batch of response signals is used, especially under complicated boundary conditions or if multiple defective inclusions exist.

In 1986, Doctor et al. proposed the synthetic aperture focusing technique (SAFT) as a new signal processing strategy in which an ultrasonic method is used for analyzing metallic materials [11]. A conventional ultrasonic pulse-echo probe was used to generate ultrasonic waves and subsequently receive the reflected signals. Results exhibiting a high signal-to-noise (S/N) ratio were often obtained by shifting and superposing the response signals recorded using a series of pulse-echo operations. Subsequent studies have detected defects in concrete elements by using the ultrasonic SAFT [12,13]. In 2001, Krause et al. used an ultrasonic array system to image pipes located in concrete elements [14]. Although these papers presented favorable results, they cannot be applied to detect deep defects in an in situ concrete element because of the high attenuation of propagating ultrasound in concrete. Recently, some researchers used an ultrasonic tomography method to detect defects inside concrete and reinforced concrete elements and obtained good results [15–17]. It is fast and couplant-free to generate an image by using ultrasonic array and incorporated software. However, the cost of instrument is still more expensive than conventional point-source/point-receiver systems. In 2007, Tong et al. proposed an elastic-wave-based method in which the point-source/point-receiver scheme and SAFT are combined to observe the defects in a concrete element

* Corresponding author. Tel.: +886 912053833; fax: +886 3 4279351.
E-mail addresses: jhtong@sunrise.hk.edu.tw (J.-H. Tong), clchiu0907@gmail.com (C.-L. Chiu), cywang@cc.ncu.edu.tw (C.-Y. Wang), shutao@chu.edu.tw (S.-T. Liao).

http://dx.doi.org/10.1016/j.ndteint.2014.08.001
0963-8695/

in images [18]. By using mechanical impact as a wave generator, the functioning depth was substantially enhanced compared with that observed using the conventional method, in which pulse-echo probes are used for imaging defects inside concrete structures. Furthermore, Tong et al. used the SAFT to process the received signals to obtain high S/N ratio results and thereby produce high-quality images for exposing the defects in concrete structures. In 2010, they proposed a method for improving the SAFT by using Hilbert–Huang transform to enhance the quality of the resultant images [19]. Although the influence of the reflection from rebars was not discussed extensively, this is typical when inspecting reinforced concrete structures in situ. In the present study, the influence of rebars on generating SAFT images was explored using both numerical simulation and experimental methods. The results can be used as guidelines for researchers or NDT operators in selecting the source by which the introduced stress waves are generated when applying the elastic-wave-based SAFT to expose the defects in concrete structures.

2. Principle of the synthetic aperture focusing technique

When inspecting concrete structures by using the elastic-wave-based SAFT, the resultant image is similar to that obtained using a phased array system. The test is typically performed using only one point-source/point-receiver set each time, making the apparatus much more simple to use than a phased array system. Fig. 1 shows that a series of impact-and-receive operations was performed on the upper surface of the tested specimen. Let S_i and R_i denote the locations of the source and the receiver used in the i-th impact-and-receive operation, respectively. Furthermore, let $T_i(t)$ be the response trace recorded at R_i during this operation. Based on geometric design, the specimen can be meshed into grids, as shown in Fig. 1. An image intensity $I(m,n)$ can be assigned to each grid G according to the following calculation:

$$I(m,n) = \frac{1}{N}\sum_{i=1}^{N} T_i(t_i), \quad t_i = \frac{|\overrightarrow{S_iG}| + |\overrightarrow{GR_i}|}{C_P} \tag{1}$$

where m and n represent the row and column in which the grid is located in the mesh, respectively, N is the total number of obtained response traces, and C_P is the propagating velocity of the longitudinal wave. The image intensity I corresponding to each grid is determined by summing the amplitude of each trace at time t_i and then calculating the average value. Finally, the grayscale images obtained can be displayed using the optimal brightness levels on a computer screen for each grid according to its image intensity. After this image-processing procedure, the defects and interfaces in the matrix material can be exposed. In this study, abnormalities or discontinuous interfaces with high image intensity were displayed in bright white, whereas a uniform matrix with low image intensity was displayed in deep black.

3. Influence of rebars on synthetic aperture focusing technique images

To determine the influence of rebars on SAFT images, a finite difference program for solving 2-D plane-stress problems was used as a numerical simulation tool. In this study, the Lamé constants, λ and μ, and the mass density used for concrete were 6.890×10^9 N/m^2, 1.379×10^{10} N/m^2, and 2300 kg/m^3, respectively. For rebars, they were 6.436×10^{10} N/m^2, 8.030×10^{10} N/m^2, and 7700 kg/m^3. To simulate the free fall of a steel ball of radius R from a height of H onto the top surface of the specimen, the impacting force was simulated using a point load in the form of a half cycle of the function $\sin^{3/2}(t)$. The reason for using this function is based on

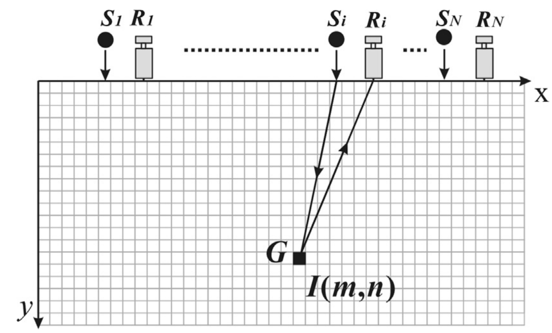

Fig. 1. Schematic showing impact-and-receive operations and meshing of specimen for image processing with SAFT.

the fact that it fits well with the history curve of an impact force in situ. The duration T_c of the impact can be estimated using the following equation which was derived on the basis of Hertz contact theory [10]. Let E_1 and ν_1 denote Young's modulus and Poisson's ratio of the steel ball, and E_2 and ν_2 denote Young's modulus and Poisson's ratio of the concrete. The duration of the impact between the steel ball and the concrete is estimated as

$$T_c = 5.97[\rho_1(\delta_1+\delta_2)]^{2/5}\frac{R}{H^{1/10}} \tag{2}$$

where

$$\delta_1 = \frac{1-\nu_1^2}{\pi E_1}, \qquad \delta_2 = \frac{1-\nu_2^2}{\pi E_2}$$

This equation also indicates that the contact time T_c of the impact is mainly dependent on the size of the steel ball and is proportional to its radius R. Once the duration is determined, the dominant wavelength of the elastic wave introduced by the impact force may be estimated by $1/(2T_c)$. It should be noted that the frequency contents of the introduced stress waves may range widely due to the impact force, and therefore the dominant frequency should be determined in the frequency domain. However, the value$1/(2T_c)$ is quite a good estimate from experience. To study the effect of the wavelength of the elastic stress wave introduced by the impact of steel ball, various sizes of steel spheres with different diameters were used in this research. They were 8, 10, 12.7, 15.9, and 19.1 mm. Among them, the research results associated with 10-mm and 19.1-mm steel spheres were presented in the paper because they were good examples representative of crucial cases when the dominant wavelength of the elastic stress wave is 236 mm or 454 mm, which is as short as 10 times of the diameter of the rebar or as long as 20 times of it.

3.1. Resultant image of a plain concrete specimen with a single defect

A concrete plate with a void defect was used in this simulation. The plane views of such a plate without and with a layer of rebars are shown in Fig. 2(a) and (b), respectively. A series of impact-and-receive operations was performed on the top surface of the block. The impact was simulated using a half cycle of the force–time history $\sin^{3/2}t$ with a contact duration of 30.7 μs, resulting in an elastic wave with a dominant wavelength of 236 mm. The response signals were recorded using a nearby receiver on the surface for a subsequent process. In this scenario, the first impact S_1 was applied 700 mm from the left side of the block. The distance between the impacting source and the receiver was fixed at 50 mm. After a trace was recorded, the testing set was moved to the right by 25 mm for the next operation.